LA-UR-97-5089

Title: NEUTRON RESONANCES IN THE COMPOUND NUCLEUS: PARITY NONCONSERVATION TO DYNAMIC TEMPERATURE MEASUREMENTS

CONF-970845--

Author(s): VINCENT W. YUAN

Submitted to: INTERNATIONAL CONFERENCE ON PHYSICS SINCE PARITY SYMMETRY BREAKING, A CONFERENCE IN MEMORY OF PROFESSOR C. S. WU (NANJING, CHINA 1997)

Los Alamos
NATIONAL LABORATORY

NEUTRON RESONANCES IN THE COMPOUND NUCLEUS: PARITY NONCONSERVATION TO DYNAMIC TEMPERATURE MEASUREMENTS

V. YUAN
Los Alamos National Laboratory, Physics Division, MS H803, Los Alamos NM 87545, USA
E-mail: vyuan@lanl.gov

Experiments using epithermal neutrons that interact to form compound-nuclear resonances serve a wide range of scientific applications. Changes in transmission which are correlated to polarization reversal in incident neutrons have been used to study parity nonconservation in the compound nucleus for a wide range of targets. The ensemble of measured parity asymmetries provides statistical information for the extraction of the rms parity-violating mean-square matrix element as a function of mass. Parity nonconservation in neutron resonances can also be used to determine the polarization of neutron beams. Finally, the motion of target atoms results in an observed temperature-dependent Doppler broadening of resonance line widths. This broadening can be used to determine temperatures on a fast time scale of one microsecond or less.

1 Introduction

Epithermal neutron resonances have a wide range of scientific applications to both basic and applied physics research. At the Los Alamos Neutron Science Center (LANSCE), resonances formed with polarized neutrons can be used to study fundamental symmetries in the nucleon-nucleon interaction. Large enhancements to observable asymmetries in parity nonconservation (PNC) can result from high level densities in compound nuclei and from different P-wave and S-wave decay amplitudes [1,2]. These enhancements can result in PNC asymmetries that are as large as 10% [3,4,5]. For a given target, experimental techniques now allow PNC asymmetries to be measured in many resonances When statistical methods are applied to the ensemble of measurements, one can extract M, the root-mean-squared PNC matrix element, for S-wave and P-wave mixing in the target material studied. One can then use M to calculate a PNC spreading width, and this spreading width can be used to set limits on meson weak-coupling constants which parameterize the meson-exchange model of the nucleon-nucleon interaction.

In the last 2 years, compound-nuclear resonances have been applied to the measurement of temperatures in rapidly changing systems. Temperature is determined by the Doppler broadening of the resonance profile and measurements are possible on time scales as short as a fraction of a microsecond.

2 Parity Violation in the Compound Nucleus

To study compound-nuclear resonances, one requires both an intense source of epithermal neutrons and a method to distinguish among the interactions of neutrons possessing different energies. The high-flux neutron spallation beam at LANSCE [6] has, over the past 10 years, provided neutrons for PNC studies at Los Alamos. 800-MeV protons from the LANSCE linac are accumulated in a proton storage ring and then targeted in short (250-ns-wide) pulses onto a tungsten spallation target. High-energy neutrons produced in spallation interactions are moderated in H_2O to produce the .1 to 1000 eV neutrons used in neutron resonance experiments. Neutrons of a particular energy exit the moderator with a tail containing time decays of [7] $.99/E^{.37}\mu s$ and $3.9/E^{.37}\mu s$. The moderated neutrons traverse the experimental flight path in a time that is inversely proportional to their velocity. Detectors are coupled to a transient digitizer and scan a time interval which can be altered in length (between 800 μs and 8 ms) so as to detect the neutron arrival as a function of time. The time of neutron arrival is used to determine neutron energy.

In the apparatus for measuring PNC in neutron resonances, epithermal neutrons are passed through a cryogenic polarized-proton spin filter [8] which polarizes the neutrons by selective transmission of neutrons with spin alignment parallel to that of protons in the filter. The neutrons emerge polarized longitudinally, in other words with spins either parallel or anti-parallel to their direction of motion. A region of combined fixed-longitudinal and varying-transverse magnetic fields (spin flipper [9]) permits the neutron spin to either be reversed in direction (flip) or to pass unaltered (noflip). For transmission experiments, target samples are placed at the exit of the spin-flipper. If sample rarity makes it difficult to obtain a thick enough target for a transmission measurement, then PNC measurements can be conducted in capture-gamma mode [10] with thin samples placed at the detector.

2.1 Classes of PNC experiments

PNC in hadronic interactions is a way to study the contribution from the weak force to nucleon-nucleon interactions. A way of characterizing the interaction between two nucleons is through the exchange of mesons. Such a coupling is customarily modeled with a strong-interaction vertex at one nucleon and a weak-interaction vertex at the other nucleon. One goal of PNC experiments is to determine the weak meson-exchange coupling constants that parameterize the meson exchanges [11].

PNC experiments can be divided into several classes. The simplest systems studied fall in the category of 'few-body' interactions. In these systems, such as $\vec{p} + p$ scattering or $\vec{n} + p \rightarrow d + \gamma$, the interactions involve individual nucleons, and nuclear structure plays a minimal role. Without nuclear structure effects, results are often simplest to interpret, but observed PNC effects remain unmagnified. These small PNC effects can be difficult to measure and are susceptible to contributions from systematic errors. An example showing the size of a successful measurement of PNC in this type of experiment is the result from $p \vec{+} p$ scattering at 45 MeV[12]: $A_L = -(1.50 \pm .22) \times 10^{-7}$.

Nuclear-structure enhancements, which are present in PNC experiments in light nuclei (such as in ^{18}F, ^{19}F, and ^{21}Ne), can result in asymmetries that are several orders of magnitude larger than those of the few-body experiments. For example, the observed PNC effect in the ^{19}F experiment[13] is $A_L = -(7.4 \pm 1.9) \times 10^{-5}$. While observed effects may be larger, the interpretation of results becomes more difficult because the contributions of nuclear structure must be calculated.

Experiments which measure PNC in compound-nuclear resonances are conducted in medium to heavy nuclei (A=100 to A=238). These systems possess complicated nuclear structures - making it difficult to interpret the measured PNC asymmetries of individual resonances. If, however, PNC asymmetries can be measured in a large number of resonances, then statistical methods can be applied to determine M, the root-mean-squared PNC matrix element. From M one can determine the PNC spreading width Γ_{PNC} which is given by[14]

$$\Gamma_{PNC} = 2\pi \frac{M^2}{D} \tag{1}$$

where D is the level spacing.

2.2 Systematics

The LANSCE PNC experiments[15] are designed to minimize the contribution of systematics. Data is retaken one-sixtieth of a second after the passage of each neutron pulse and subtracted from the raw signal in order to eliminate the contribution of 60-Hz noise. An eight-step polarization reversal pattern (+−+-++-) is employed to eliminate the contribution of slow drifts. When neutron spins are reversed, the motion of the spins are processed alternately in clockwise and counterclockwise directions in order to eliminate any net contributions from the transverse fields of the spin flipper. The sum total of systematic contributions has been determined by measuring the PNC asymmetry seen in parity-conserving S-wave impurity resonances, and was found to be less than 1 part in 10^5.

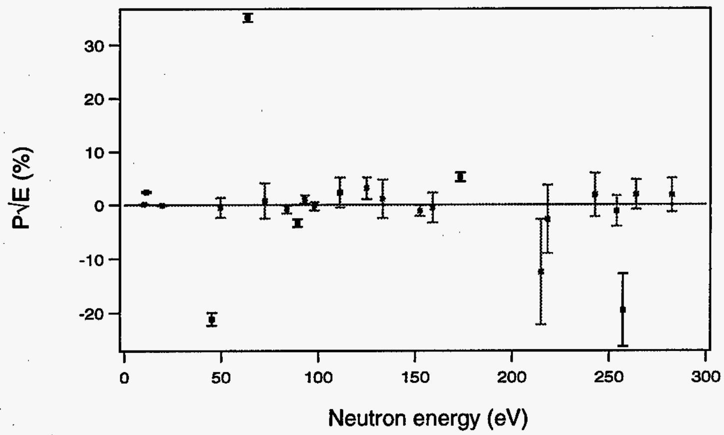

Figure 1: PNC asymmetry data for ^{238}U.

2.3 PNC results

At LANSCE, PNC has been measured over numerous resonances in targets of ^{104}Pd, ^{105}Pd, ^{106}Pd, ^{107}Ag, ^{108}Pd, ^{109}Ag, ^{113}Cd, ^{115}In, ^{117}Sn, ^{127}I, ^{232}Th, and ^{238}U. As a representative example, Figure 1 shows the measured [7] $P\sqrt{E}$ value for the resonances in ^{238}U. Six of the helicity-dependent asymmetries are significantly non-zero by more than 2.5 σ.

For any target sample, the measured PV in the i^{th} p-wave resonance is given by

$$P_i = 2\sum_j \frac{<\psi_P^i|V|\psi_S^j>}{E_S^j - E_P^i}\sqrt{\frac{\Gamma_S^{n,j}}{\Gamma_P^{n,i}}} = \sum_j V_{ij}A_{ij} \tag{2}$$

where $V_{ij} =<\psi_P^i|V|\psi_S^j>$; $\psi_P^i, E_P^i, \Gamma_P^i$ are the wavefunction, energy, and neutron decay width of the p-wave resonance and $\psi_S^j, E_S^j, \Gamma_S^j$ are the corresponding quantities for each of the j s-wave resonances that contribute to the PNC mixing. The statistical model of the compound nucleus [16,17] assumes that each PNC matrix element $V_{ij} =<\psi_P^i|V|\psi_S^j>$ is drawn from Gaussian-distributed random variables with mean =0 and variance = M^2. Then from the ensemble of measured P_i values for a given sample, a value of M can be extracted through the construction of a likelyhood function [18,19].

Because PNC mixing must occur between s-wave and p-wave resonances of equal total spin J, not every p-wave resonance is capable of exhibiting PNC

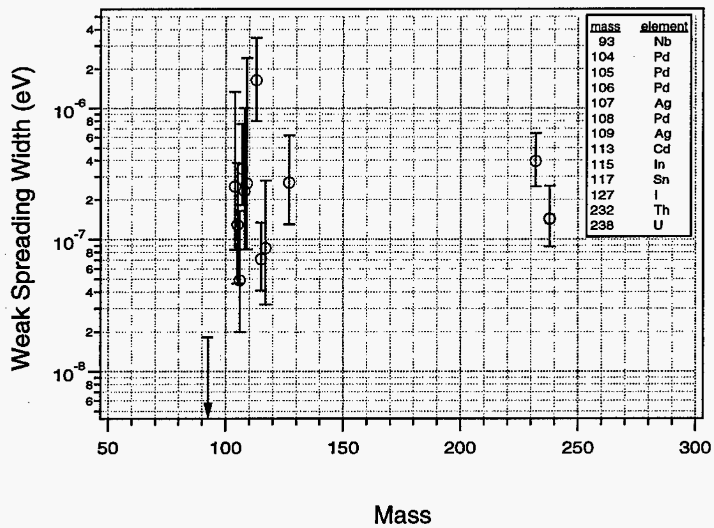

Figure 2: Weak spreading width as a function of target mass. The measurement for ^{93}Nb gives an upper limit.

mixing. For instance in I=0 nuclei, J=1/2 s waves can mix with j=1/2 p waves, but not with j=3/2 p waves. The likelyhood function for p-wave resonances in I=0 target nuclei is given by

$$L(M) = \prod_{i=1}^{n}\{\frac{1}{3\sqrt{2\pi(\sigma_{Q_i}^2 + M^2)}}e^{\frac{-Q_i^2}{2(\sigma_{Q_i}^2+M^2)}} + \frac{2}{3\sqrt{2\pi\sigma_{Q_i}^2}}e^{\frac{-Q_i^2}{2\sigma_{Q_i}^2}}\} \tag{3}$$

where $Q_i = P_i/\sum_j A_{ij}$ and the 2 terms contained in the curly braces represent contributions where mixing respectively can and cannot occur.

Measurements of PV have been made in targets clustered near A=100 and A=238. Figure 2 shows that Γ_{PNC} exhibits a weak, if any, dependence on target mass.

2.4 Limits on Meson Coupling Constants

The value of M^2 can be related[20] to the pion and rho meson coupling constants F_π and h_ρ by the relation

$$M^2 = \alpha(A)F_\pi^2 + \beta(A)F_\pi h_\rho + \gamma(A)h_\rho^2 \tag{4}$$

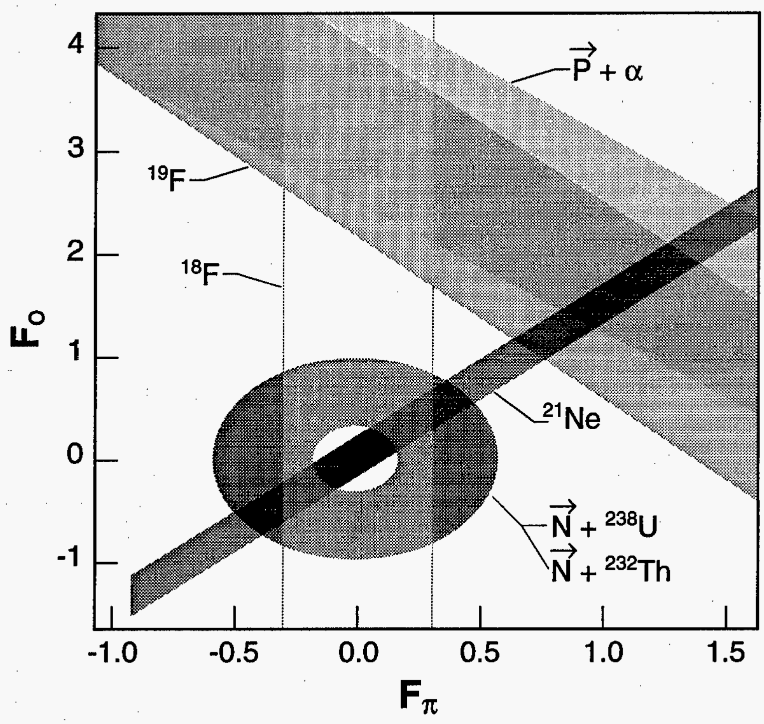

Figure 3: Constraints (donut-shape) on meson coupling constants F_π and h_ρ that result from the determination of M^2. Also shown on plot are constraints that result from other experiments.

where the coefficients $\alpha(A)$, $\beta(A)$, and $\gamma(A)$ are determined using the statistical model of the compound nucleus. Because Johnson *et. al.* found the cross term to be negligible, the constraints to F_π and h_ρ can be represented in the form of a donut in F_π, h_ρ space (see figure 3). The constraints represented in figure 3 are based on early PNC data comprising a small subset of the present full data set. Work is presently being carried out to revise the constraints, and it is expected [21] that the new constraints will result a new donut possessing a width approximately 20% of its radius.

3 Measuring Polarization

To extract the PNC asymmetry P from measured helicity-dependent transmissions, one must accurately know the absolute polarization of the neutron beam.

Consider a neutron beam with polarization $f_n = \frac{N_{\rightarrow} - N_{\leftarrow}}{N_{\rightarrow} + N_{\leftarrow}}$ passing through an unpolarized target. Here $N_{\rightarrow}(N_{\leftarrow})$ refers to the number of neutrons with spin forward (backward). The helicity dependence of neutron transmission through the target is given [5] by two yield expressions

$$Y_{flip} = N_0 C(E) e^{-\sigma(E)t(1-f_n P)} \tag{5}$$

$$Y_{noflip} = N_0 C(E) e^{-\sigma(E)t(1+f_n P)} \tag{6}$$

which depend explicitly on f_n. Hence f_n must be accurately determined before an accurate value of P can be extracted from the measurement.

In the LANSCE experiments, neutrons are polarized by passage through a polarized proton target [8,15]. Neutrons with spins parallel to the polarized-proton spin direction are preferentially transmitted over neutrons with spins oriented anti-parallel to that of the protons. The total number of neutrons transmitted depends on the mix of forward-directed and backwards-directed proton spins. Hence, one can use transmission to accurately determine polarization [5], provided that the polarizing crystals are uniformly polarized. But non-uniformities in the polarizer can result in an erroneous determination of f_n [5].

The LANSCE experiments presently determine neutron polarization using a method based on the double-lanthanum parity measurement [5]. In this experiment, which measures PNC in a ^{139}La target, the polarized proton spin filter is replaced with a second Lanthanum sample which polarizes the incident neutron beam via PNC in the weak interaction. Though it is not an efficient means of polarization, this method leads to a determination of P which does not explicit depend on f_n. The asymmetry value from this experiment, $P = .0955 \pm .0035$, is used to calibrate simultaneously-made double-Lanthanum and NMR measurements to each other.

4 Neutron Resonance Spectroscopy (NRS)

In the last two years, neutron resonances have emerged as a means of making dynamic temperature measurements in the field of Shock Physics [22]. The term 'dynamic' here refers to a system which is changing rapidly, and in such a system temperature measurements are sought on a very fast timescale - a timescale on the order of 1 μ s or less. Temperatures in NRS are determined by measuring the Doppler broadening of the resonance lineshape. Such a broadening is the result of the thermal motion of atoms in the target. NRS has advantages over other techniques because it is both non-invasive and can probe

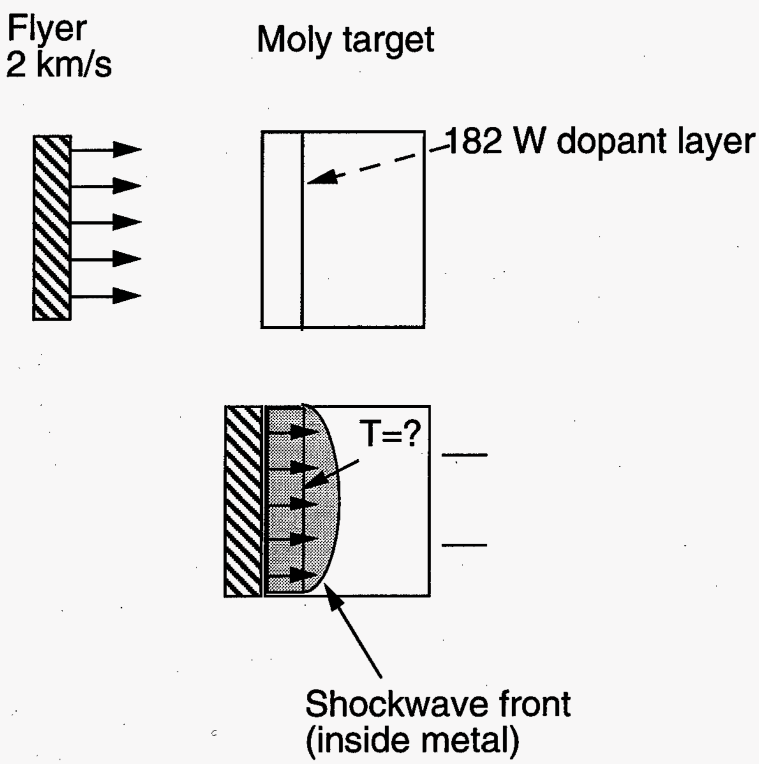

Figure 4: Schematic of Temperature Behind Shock Experiment

the interior of the sample. An example of an NRS application is measuring the temperature in a metal immediately after the passage of a shock wave. Figure 3 shows schematically an aluminum flyer plate which induces a shockwave in a molybdenum target. Inside the target is a thin layer of ^{182}W which provides a resonance (21.1 eV) which will be broadened by the temperature rise in the molybdenum. Once the induced shock has passed the dopant layer of W, the measurement must be made in the short time window that exists before the rarefaction waves return approximately 1μ s later from the surfaces of the sample and change the conditions of the shocked interior.

Temperature measurements can be made on a timescale of the transit time for neutrons of the resonance to pass through the sample. For a resonance of

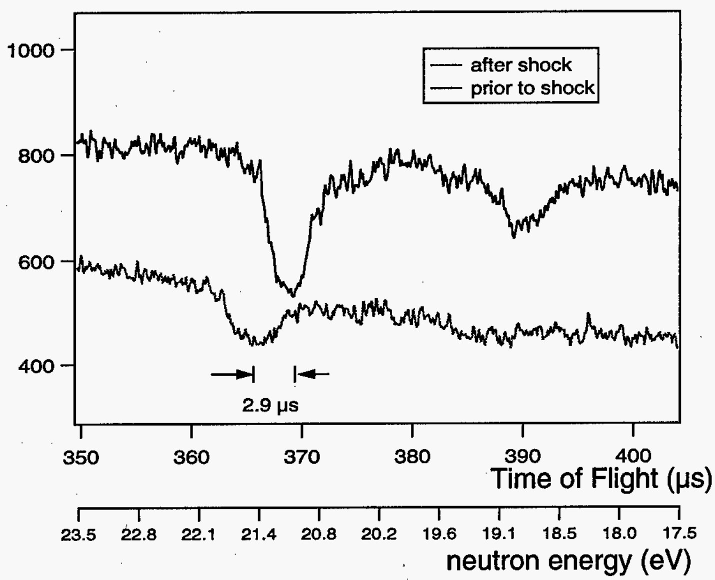

Figure 5: 21.1-eV resonance in ^{182}W prior to and after passage of shockwave.

width ΔE, this transit time is given by

$$\Delta t = \frac{t\Delta E}{2E} \quad . \tag{7}$$

In the case of the 21.1-eV neutrons passing through a ^{182}W sample located 1m from the neutron source, Δt is approximately 170 ns.

If one assumes a Maxwell-Boltzmann distribution of velocity for atoms in the target, then the Doppler contribution to the resonance width is given by

$$\Delta E = \sqrt{\frac{2E_n kT}{A}} \tag{8}$$

where E_n is the neutron energy, T is the temperature, and A is the target mass.

4.1 NRS example

Results from an experiment to measure the temperature in shocked molybdenum are shown in Figure 4. The curves show before-shock and after-shock profiles of the ^{182}W, 21.1-eV resonance from the dopant layer inside the shocked molybdenum. One can see that the after-shock profile (bottom curve) is both broader than the unshocked profile (top curve) and Doppler shifted to higher energy. Analysis is currently being performed to determine the precise temperature of the shocked molybdenum.

5 Summary

High-intensity neutron spallation sources and time-of-flight methods can be used to study neutron resonance spectra in the compound nucleus. The use of these neutron resonances can be applied to a wide range of disciplines ranging from nuclear physics to shock physics. In nuclear physics, neutron resonances have been successfully applied over a 10 year period to studying PNC in the nucleon-nucleon interaction. The applications to shock physics are just beginning to be realized with NRS use in making dynamic temperature measurements.

References

1. O. P. Sushkov and V. V. Flambaum, *Sov. Phys. Usp* **25**(1), 1 (1982).
2. V. E. Bunakov and V. P. Gudkov, *Nucl. Phys* **A401**, 93 (1983).

3. V. P. Alfimenkov, S. B. Borzakov, Vo Van Thuan, Yu. D. Mareev, L. B. Pikelner, A. S. Khrykin, and E. I. Sharapov, *Nucl. Phys.* **A398**, 93 (1983).
4. Y. Masuda, T. Adachi, A. Masaike, and K. Morimoto, *Nucl. Phys.* **A504**, 269 (1989).
5. V. W. Yuan, C. D. Bowman, J. D. Bowman, J. E. Bush, P. P. J. Delheij, C. M. Frankle, C. R. Gould, D. G. Haase, J. N. Knudson, G. E. Mitchell, S. I. Penttilä, H. Postma, S. J. Seestrom, J. J. Szymanski, and X. Zhu, *Phys. Rev.* C **44**, no. 5, 2187 (1991).
6. P. W. Lisowski, C. D. Bowman, G. J. Russell, and S. A. Wender, *Nuclear Science and Engineering* **106**, 208 (1990).
7. B. E. Crawford, *Ph. D. Thesis*, Dept. of Physics, Duke University 1997.
8. S. Penttilä, J. D. Bowman, P. P. J. Delheij, C. M. Frankle, D. G. Haase, R. N. Mortensen, H. Postma, S. J. Seestrom, and Yi-Fen Yen, in *Time Reversal Invariance and Parity Violation in Neutron Reactions*, 198 (Dubna, Russia, 1993).
9. J. D. Bowman, S. I. Penttilä, and W. B. Tippens, *Nucl. Instr. and Meth.* **A369**, 195, (1996).
10. B. E. Crawford, J. D.Bowman, C. M. Frankle, T. Haseyama, A. Masaike, Y. Matsuda, S. I. Penttilä, N. R. Roberson, S. J. Seestrom, E. I. Sharapov, and S. L Stephenson, in *Fourth International Seminar on Neutron-Nucleus Interactions*, 268 (JINR, Dubna, 1996).
11. B. Desplanques, J. F. Donoghue, B. R. Holstein, *Ann. Phys.* **124**, 449 (1980).
12. S. Kistryn, J. Lang, J. Liechti, Th. Maier, R. Müller, F. Nessi-Tedaldi, M. Simonius, J. Smyrski, S. Jaccard, W. Haeberli, and J. Sromicki, *Phys. Rev. Lett.* **58**, no. 16, 1616 (1987).
13. E. G Adelberger and W. C. Haxton, *Ann. Rev. Nucl. Part. Sci.* 1985 **35**, 501.
14. V. E. Bunakov, in *Parity and Time Reversal Violation in Compound Nuclear States and Related Topics*, 113 (Trento, Italy, 1995).
15. N. R. Roberson, C. D. Bowman, J. D. Bowman, P. P. J. Delheij, C. M. Frankle, C. R. Gould, D. G. Haase, J. N. Knudson, G. E. Mitchell, R. N. Mortensen, S. I. Penttilä, H. Postma, S. J. Seestrom, J. J. Szymanski, S. A. Wender, S. H. Yoo, V. W. Yuan and X. Zhu, *Nucl. Instr. and Meth.* **A326**, 549 (1993).
16. J. D. Bowman, C. D. Bowman, J. E. Bush, P. P. Delheij, C. M. Frankle, C. R. Gould, D. G. Haase, J. N. Knudson, G. E. Mitchell, S. I. Penttilä, H. Postma, N. R. Roberson, S. J. Seestrom, J. J. Szymanski, V. W. Yuan, and X. Zhu, *Phys. Rev. Lett.* **65**, 1192 (1990).

17. V. E. Bunakov, E. D. Davis, and H. A. Weidenmüller, *Phys. Rev.* **C42**, 1718 (1990).
18. J. D. Bowman, L. Y. Lowie, G. E. Mitchell, E. I. Sharapov, and Y.-F. Yen, *Phys Rev* C**53**, 285 (1996).
19. J. D. Bowman, L. Y. Lowie, E. I. Sharapov, Phys. Part. Nucl. **27**, 398 (1996).
20. M. B. Johnson, J. D. Bowman, and S. H. Yoo, *Phys. Rev. Lett.*, **67**, 310 (1991).
21. J. D. Bowman, *private communication* (1997).
22. V. W. Yuan, B. W. Asay, R. Boat, J. D. Bowman, D. J. Funk, R. Hixson, L. Hull, G. Laabs, R. Lonson, G. L. Morgan, R. Rabie, and C. E. Ragan, to be published in *Proceedings of International Conference on Nuclear Data for Science and Technology, NDST '97*, (Trieste, 1997).

M98004212

Report Number (14) LA-UR--97-5089
CONF-970845--

Publ. Date (11) 199708
Sponsor Code (18) DOE/ER, XF
UC Category (19) UC-413, DOE/ER

DOE